

Constraints on Galaxy Evolution and the Cosmological Constant From Damped Ly α Absorbers

Eric Woods¹ and Abraham Loeb²

Astronomy Department, Harvard University, 60 Garden St., Cambridge, MA 02138

ABSTRACT

We use the existing catalog of Damped Lyman–Alpha (DLA) systems to place constraints on the amount of evolution in the baryonic content of galaxies and on the value of the cosmological constant. The density of cold gas at redshifts $z = 3 \pm 1$ is obtained from the mean HI column density of DLAs per cosmological path length. This path length per unit redshift is in turn a sensitive function of the vacuum density parameter, Ω_Λ . We compare the total inferred mass of cold gas at high redshifts to that observed in stars today for cosmologies with $\Omega_m + \Omega_\Lambda = 1$, where Ω_m is the matter density parameter. We define η to be net fraction of the baryonic content of local galaxies which was expelled since $z = 3$, and use Bayesian inference to derive confidence regions in the (η, Ω_Λ) plane. In all cosmologies we find that $\eta < 0.4$ with at least 95% confidence if $< 25\%$ of the current stellar population formed before $z = 3$. The most likely value of η is negative, implying a net *increase* by several tens of percent in the baryonic mass of galaxies since $z = 3 \pm 1$. On the other hand, recent observations of high metal abundances in the intracluster medium of rich clusters (Loewenstein & Mushotzky 1996) require that metal–rich gas be *expelled* from galaxies in an amount approximately equal to the current mass in stars. Based on our results and the low metallicity observed in DLAs at $z \gtrsim 2$, we infer that more than half of the baryonic mass processed through galaxies must have been assembled and partly expelled from galaxies *after* $z = 2$. We expect our constraints to improve considerably as the size of the DLA sample will increase with the forthcoming Sloan Digital Sky Survey.

Subject headings: cosmology: theory – quasars: absorption lines – galaxies: formation

Submitted to *The Astrophysical Journal*, March 1997

¹email: ewoods@cfa.harvard.edu

²email: aloeb@cfa.harvard.edu

1. Introduction

To date, some ~ 80 Damped Lyman-Alpha (DLA) absorption systems have been identified in the spectra of high-redshift QSOs. The observed absorption troughs indicate concentrations of neutral gas, with large HI column densities, $N \gtrsim 10^{20} \text{ cm}^{-2}$. There is considerable evidence that these objects are associated with the progenitors of present-day galaxies. This has been confirmed in several cases by direct imaging of QSO fields (Steidel et al. 1994, 1995, 1996; Djorgovski et al. 1996; Le Brun et al. 1996). There are various indications that DLAs are associated with young galaxies. The abundances of metals at low ionization stages in DLAs are comparable to those found in disk galaxies (Wolfe 1995). The metal absorption line profiles show a leading-edge asymmetry (Wolfe 1995; Prochaska & Wolfe 1997) and are shifted relative to the Ly α emission redshift (Lu, Sargent, & Barlow 1997), as expected from a rotating thick disk with circular velocities comparable to those seen in spiral galaxies. Furthermore, observations of redshifted 21-cm absorption and emission from DLAs indicate disk-like structures of galactic dimensions (Briggs et al. 1989; Wolfe et al. 1992). However, recent HST images (Le Brun et al. 1996) have revealed that DLA galaxies span a wide range of morphological types. The existence of a substantial galaxy population at redshifts $z \gtrsim 2$ is consistent with most CDM models, which predict that galaxies should form by $z \approx 2 - 3$ (Frenk et al. 1996, and references therein).

The HI column densities in DLAs can be derived from the equivalent widths of the observed absorption features. The mean HI column density along a random line of sight may then be summed up and divided by the absorption path length probed to obtain the comoving spatial HI mass density ρ_{HI} in galaxies at a given redshift. Since DLAs dominate the HI mass in the universe (Lanzetta et al. 1995, and references therein), their statistics can be used to infer the evolution of the comoving HI density from high redshifts up to the present epoch. Recent work (Lanzetta et al. 1995; Wolfe et al. 1995; Storrie-Lombardi, McMahon, & Irwin 1996) has shown that, for universes with a zero cosmological constant ($\Lambda = 0$), the inferred comoving total gas density $\rho_{\text{g}} = 1.3\rho_{\text{HI}}$ (including HI and He) at a redshift $z \approx 3.5$ is comparable to the stellar mass density observed in present-day galaxies. This was seen to be consistent with a simple “closed-box” picture in which galaxies had formed by $z = 3.5$, and the neutral gas was subsequently converted into stars, while the total baryonic mass (gas + stars) is conserved. Note that the closed-box model does not assume that the baryonic masses of individual galaxies are conserved but rather that the total baryonic mass of *all* galaxies is not evolving with time. This model allows for mergers which conserve the total mass of all of the galaxies involved.

Evolutionary models may be generalized to include a net infall of gas from the intergalactic medium, or a net outflow of gas from DLA galaxies. The closed-box assumption represents the simplest evolutionary model, but in general we do not expect the total baryonic mass in galaxies to be conserved. In particular, the intracluster medium (ICM) in rich clusters of galaxies contains an amount of iron which is approximately equal to the amount locked in stars in these clusters (Renzini et al. 1993; Loewenstein & Mushotzky 1996). The natural explanation is that the metals observed in the ICM were produced inside of galaxies and subsequently expelled into the ICM by

supernova-driven winds. In this paper, we examine whether the DLA data are consistent with the substantial outflow needed to account for this observation.

In the subsequent discussion, we also allow $\Lambda \neq 0$, and explore the family of models with $\Omega_m + \Omega_\Lambda = 1$, where Ω_m and Ω_Λ are the mean present-day cosmic mass densities in matter and vacuum energy, respectively, in units of the critical density. The absorption path length corresponding to a given redshift interval depends on the assumed cosmological model; it is shortest for flat, $\Lambda = 0$ universes, longer for open, $\Lambda = 0$ universes, and longer still for flat, $\Lambda \neq 0$ models. Because the absorption path length is longest for Λ -dominated cosmologies, we expect the inferred value of ρ_g at high redshifts to be the smallest, and hence the deficit with respect to the present-day stellar density to be the largest in these cosmologies. This approach is similar to methods which constrain Ω_Λ based on the statistics of gravitational lensing (Kochanek 1996, and references therein). In closed-box models, one may investigate the constraints that can be placed on Ω_Λ by requiring, for some suitably chosen $z > 2$, that $\rho_g(z)$ be comparable to the present-day mass density in stars, $\rho_s(0)$. However, a net infall of gas between the high-redshift epoch and $z = 0$ can bring the DLA data into reasonable agreement with high- Λ cosmologies. For our purposes, it is sufficient to parameterize the amount of accretion or expulsion as $\eta \equiv \rho_{b,\text{gal}}(z)/\rho_{b,\text{gal}}(0) - 1$, where $\rho_{b,\text{gal}} = \rho_g + \rho_s$ is the total baryonic density in galaxies, and $\rho_{b,\text{gal}}(0) \approx \rho_s(0)$. In this paper we explore the constraints on both galaxy evolution and cosmology by constructing confidence regions in the (η, Ω_Λ) plane. To simplify our analysis, we make the reasonable assumption that the distribution of DLAs in HI column density N and redshift z , $F(N, z)$, is separable into functions of N and z over a suitably small redshift interval. This allows us to fit the column density distribution separately from the extraction of constraints on galaxy formation or the underlying cosmology [the latter being exclusively related to the redshift dependence of $F(N, z)$].

The value of $\rho_s(0)$ is calculated by multiplying the local luminosity density by the mean mass-to-light ratio. Recent imaging of DLA galaxies (Le Brun et al. 1996) indicates that, while some are spirals, a significant fraction of these objects have irregular morphologies, which may indicate that a substantial amount of merging was taking place at high redshifts. Since mergers may result in the formation of elliptical galaxies, we include all galaxy types in our calculation of the local luminosity density, and hence $\rho_s(0)$. The assumption that underlies our discussion is that star formation requires *cold* HI gas, which must be represented in a fair sample of all Ly α absorption systems, irrespective of whether the star formation process occurs in spirals or in ellipticals.

In §2.1 we show how the comoving HI density is inferred from the DLA sample, and how sensitive it is to the underlying cosmology. Section 2.2 adds the impact that evolution in the HI content of galaxies might have on our analysis. In §3 we discuss the statistical methods used to compare the data to the theoretical predictions for $\rho_g(z)$. In §4 we present the derived confidence intervals for our constraints on the evolution of galaxies and the cosmological constant. Finally, §5 summarizes our conclusions.

2. Evolution Of The Comoving HI Density

In order to extract useful constraints from the data, we must predict some observable property of the DLA sample, and show explicitly how our prediction depends on our assumptions about cosmology and evolution. In §2.1, we show how, for a given cosmology, the comoving HI density $\rho_{\text{HI}}(z)$ is related to the total DLA column density along a line of sight. In §2.2, we introduce a parameter which characterizes the amount of evolution in the HI density.

2.1. Inferring $\rho_{\text{HI}}(z)$ from the DLA Sample: Effects of Cosmology

The comoving HI density in DLA systems at a redshift z is inferred by calculating the mean HI column density in a proper length interval cdt along a line of sight, and dividing the result by $(c/H_0)dX \equiv (1+z)^3 cdt$. Since the absorption path length element dX corresponding to a given redshift element dz depends on the cosmological parameters Ω_m, Ω_Λ (the mean present-day cosmic mass densities in matter and vacuum energy, respectively, in units of the critical density), the inferred value of the comoving HI density will depend on the assumed geometry of the universe. Let $F(N, z)dNdz$ be the mean number of DLAs along a line of sight with HI column densities between N and $N + dN$ and redshifts between z and $z + dz$. Note that $F(N, z)$ is different from the function $f(N, z)$ usually encountered in the literature; the latter is conventionally defined such that $f(N, z)dNdX$ gives the number of DLAs with with column densities between N and $N + dN$ and absorption distances between $X(z)$ and $X(z) + (dX/dz)dz$. The inferred comoving HI density is given by

$$\rho_{\text{HI}}(z) = \left(\frac{H_0 m_{\text{H}}}{c} \right) \left[\frac{dz}{dX}(z, \Omega_m, \Omega_\Lambda) \right] \int_{N_{\text{min}}}^{\infty} F(N, z) N dN, \quad (1)$$

where m_{H} is the mass of a hydrogen atom, and $N_{\text{min}} = 2 \times 10^{20} \text{ cm}^{-2}$ is the minimum HI column density included in the sample. For a cosmological model with density parameters $(\Omega_m, \Omega_\Lambda)$ and an open or flat geometry, the absorption path length element dX is given by

$$dX = \frac{(1+z)^2 dz}{\sqrt{\Omega_m(1+z)^3 + (1 - \Omega_m - \Omega_\Lambda)(1+z)^2 + \Omega_\Lambda}}. \quad (2)$$

For a flat matter-dominated universe with $\Omega_m = 1$ and $\Omega_\Lambda = 0$, $dX = (1+z)^{1/2} dz$; for a low-density universe with $\Omega_m = 0$ and $\Omega_\Lambda = 0$, $dX = (1+z) dz$; and for a flat, Λ -dominated universe with $\Omega_m = 0$ and $\Omega_\Lambda = 1$, $dX = (1+z)^2 dz$. Hence, because the path length corresponding to a given redshift interval dz is longest for Λ -dominated cosmologies, the $\Omega_{\text{HI}}(z)$ value inferred from equation (1) is smallest for large Ω_Λ . In this paper we will only consider the family of flat cosmologies with $\Omega_m + \Omega_\Lambda = 1$, and will write all cosmology-dependent expressions in terms of the single adjustable parameter Ω_Λ .

The *observed* distribution $F_{\text{obs}}(N, z)dNdz$, defined as the *total* number of DLAs observed in the sample with column densities between N and $N + dN$ and redshifts between z and $z + dz$,

depends on the sensitivity of the QSO sample to the detection of a DLA feature at redshift z . In the absence of obscuration of background QSOs by dust in the DLAs,

$$F_{\text{obs}}(N, z) = g(z)F(N, z), \quad (3)$$

where

$$g(z) \equiv \sum_{i=1}^m H(z_i^{\text{max}} - z)H(z - z_i^{\text{min}}). \quad (4)$$

Here, $H(x)$ the Heaviside step function, m is the total number of QSOs in the sample, and $(z_i^{\text{min}}, z_i^{\text{max}})$ is the redshift window over which the observations are able to detect a DLA feature in the spectrum of the i th QSO (depending on the redshift of the QSO and the response of the detector). Thus, $g(z)$ is the number of lines of sight for which a DLA feature is detectable at an absorber redshift z . We therefore have

$$\rho_{\text{HI}}(z) = \left(\frac{H_0 m_{\text{H}}}{c} \right) \left[\frac{\sqrt{(1 - \Omega_{\Lambda})(1 + z)^3 + \Omega_{\Lambda}}}{(1 + z)^2} \right] \frac{1}{g(z)} \int_{N_{\text{min}}}^{\infty} F_{\text{obs}}(N, z) N dN. \quad (5)$$

Equation (5) expresses the inferred value of $\rho_{\text{HI}}(z)$, factored into functions that depend exclusively on Ω_{Λ} , which we treat as a free parameter, and the properties of the QSO and DLA samples, which are fixed by observations.

2.2. Predicting $\rho_{\text{HI}}(z)$: Effects of Evolution

Given a specified galaxy evolution picture, the evolution of the gas density is obtained by solving the equations of cosmic chemical evolution (e.g. Pei & Fall 1995):

$$\dot{\rho}_{\text{g}} + \dot{\rho}_{\text{s}} = \dot{\rho}_{\text{b,gal}}, \quad (6)$$

$$\rho_{\text{g}} \dot{Z} - y \dot{\rho}_{\text{s}} = (Z_{\text{f}} - Z) \dot{\rho}_{\text{b,gal}}. \quad (7)$$

Here, the dot denotes a time derivative; ρ_{g} is the total gas density (note that $\rho_{\text{g}} > \rho_{\text{HI}}$, since ρ_{g} includes HII, H₂, He, and heavier elements); ρ_{s} is the mass density in stars; $\dot{\rho}_{\text{b,gal}}$ is the net rate at which the total baryonic mass density changes ($\dot{\rho}_{\text{b,gal}} > 0$ corresponds to a net accretion of material from the intergalactic medium, while $\dot{\rho}_{\text{b,gal}} < 0$ corresponds to a net expulsion of material from galaxies); y is the mean stellar yield (mass fraction of elements heavier than He produced in stars), averaged over the stellar initial mass function (IMF); Z is the metallicity of the gas (mass fraction of elements heavier than He present in the gas) in galaxies, and Z_{f} is the metallicity of the infalling gas. The simplest solution is the “closed-box” solution, which has no net accretion or outflow ($\dot{\rho}_{\text{b,gal}} = 0$):

$$\rho_{\text{g}}(z) = \rho_{\text{g}}(\infty) \exp \left[-\frac{Z(z)}{y} \right], \quad (8)$$

where we have assumed $Z(\infty) = 0$. Solutions which include accretion or outflow have been identified by Pei & Fall (1995) for the case where $\dot{\rho}_{\text{b,gal}} \propto \dot{\rho}_{\text{s}}$.

For simplicity, we will assume that ρ_g is constant within a sufficiently narrow redshift interval around $z = 3$. Although the minimum width of this interval is limited to $\Delta z \sim 1-2$ by the current size of the DLA sample, one can imagine that forthcoming DLA surveys will allow one to narrow it much more in the future. In principle, one could have considered the case of a constant nonzero rate of change $\dot{\rho}_g$; however, even with $\Delta z \sim 1-2$ this produces results which do not differ appreciably from the case where ρ_g is a constant, for a range of reasonable values of $\dot{\rho}_g$.

Any deficit in the gas density $\rho_g(z)$ at $z = 3$ relative to the total present-day baryonic mass $\rho_{\text{b,gal}}(0) = \rho_g(0) + \rho_s(0) \approx \rho_s(0)$ will be due to a combination of two effects: (1) some material may have accreted onto existing galaxies or assembled into new galaxies since $z = 3$, and (2) some star formation may have already occurred by redshift $z = 3$, depleting part of the gas. Effect (2) is expected to be sub-dominant based on the low metallicities $Z \sim 0.1Z_\odot$ observed at redshifts $z \gtrsim 2$ (Lu et al. 1996) and the relatively small star formation rates observed at such high redshifts (Madau 1996). Nevertheless, we will lump the two effects together, and will parameterize the combined contribution to the deficit by defining

$$\eta \equiv \frac{\rho_{\text{b,gal}}(3)}{\rho_{\text{b,gal}}(0)} - 1, \quad (9)$$

where $1 + \eta$ is the fraction of $\rho_{\text{b,gal}}(0)$ which was present at a redshift of 3. (We choose $z = 3$ as the fiducial redshift for the comparison, but since we assume that $\rho_g = \text{constant}$ over an interval containing $z = 3$, we could just as easily choose any other redshift in this interval for the definition of η .) Hence, $\eta < 0$ corresponds to a net accretion and $\eta > 0$ corresponds to a net expulsion of material since $z = 3$. Star formation prior to $z = 3$ is expected to produce at most $\sim 25\%$ of $\rho_s(0)$ (approximately the fractional area under the curve $\dot{\rho}_s(t)$ inferred from Madau 1996, corrected for high- Λ cosmologies). Let f be the fraction of the total present-day mass in stars which were produced by $z = 3 \pm 1$; then, with $\rho_{\text{b,gal}}(0) \approx \rho_s(0)$, we have

$$\rho_g(3) = (1 + \eta - f)\rho_s(0). \quad (10)$$

Finally, we neglect the contributions of ionized hydrogen, molecular hydrogen (see Ge & Bechtold 1997), as well as metals, to ρ_g at redshifts $z \gtrsim 2$, but include helium, 25% by mass, resulting in a mean molecular weight of $1.3m_{\text{H}}$. We therefore use $\rho_g = 1.3\rho_{\text{HI}}$.

3. Statistical Methods

Next we describe the methods used to compare the data to the model prediction $\rho_{\text{HI}}(z)$ for the mean HI density at high redshift, at given values of η and Ω_Λ . In §3.1, we construct the likelihood function, and in §3.2, we use Bayesian analysis to derive confidence regions in the (η, Ω_Λ) plane from the likelihood function.

3.1. Constructing a Likelihood Function

The likelihood function gives the probability of obtaining a particular data set, assuming the truth of a specified model. The model should include predictions for both the expected value of the quantity in question and the *distribution* of measurements due to statistical (e.g. Poisson) fluctuations about the expected value. The most commonly used likelihood estimator in the literature is the χ^2 statistic, which is simply proportional to the logarithm of the likelihood function for normally distributed errors. Its widespread use is due to two convenient facts: the tendency, due to the Central Limit Theorem, of sums of many random variables to be normally distributed; and the fact that the distribution of the χ^2 statistic for normally distributed errors is known, which makes it easy to calculate confidence regions. However, the χ^2 statistic is not appropriate for our analysis here. To apply the χ^2 statistic, we would need to collect the data into redshift bins, and estimate the value of ρ_{HI} in each bin by summing up the column densities and dividing by the total absorption path length probed in the bin. However, given our small sample size (only 73 objects in total), such experimentally-measured values of ρ_{HI} will not be normally distributed. In fact, the values we measured from Monte-Carlo-simulated data sets show a significant skewness in their distribution, and so we are not justified in using the χ^2 statistic to calculate confidence regions. Moreover, this approach introduces arbitrariness in the choice of bin size and also loses information about the DLA sample by binning the data. We have therefore chosen to construct a likelihood function which makes use of the *unbinned* data, and which does not rely on the assumption of normally distributed errors.

The starting point for constructing our likelihood function is to note that any prediction for $\rho_{\text{HI}}(z)$ can be related to the observed distribution of DLAs in column density and redshift using equation (5). Since we assume that $\rho_{\text{HI}}(z)$ is approximately constant over some narrow redshift interval around $z = 3$, we may use equation (10), and rearrange (5) to write

$$\int_{N_{\min}}^{\infty} F_{\text{obs}}(N, z) N dN = \left(\frac{c}{H_0 m_{\text{H}}} \right) \left[\frac{(1+z)^2 g(z)}{\sqrt{(1-\Omega_{\Lambda})(1+z)^3 + \Omega_{\Lambda}}} \right] \rho_{\text{s0}}(1 + \eta - f), \quad (11)$$

where $\rho_{\text{s0}} \equiv \rho_{\text{s}}(0)$. Thus, given an evolution model $\rho_{\text{HI}}(z)$ and a cosmological model Ω_{Λ} , we have a definite prediction for a property of the DLA sample, namely the total column density as a function of redshift [given by the left hand side of equation (11)]. Note that (11) gives the *expected* value of this quantity; it is not obvious how the values measured from hypothetical data sets should be distributed about this expected value (as mentioned above, given the small sample size, the values in each redshift bin will not be normally distributed). Specifically, the distribution of measured $\rho_{\text{HI}}(z)$ values depends on the shape of $F_{\text{obs}}(N, z)$ as a function of HI column density N , and will be skewed toward smaller values if $F_{\text{obs}}(N, z)$ is dominated by low- N systems, and vice-versa. Unfortunately, our evolution models $\rho_{\text{HI}}(z)$ predict only the first moment of $F_{\text{obs}}(N, z)$, not the distribution itself. However, the DLA sample *does* tell us something about the full distribution; in particular, the entire sample is well-fitted by a so-called gamma distribution (Storrie-Lombardi,

Irwin, & McMahon 1996):

$$F_{\text{obs}}(N, z) = F_{\star} \left(\frac{N}{N_{\star}} \right)^{-\gamma} \exp \left(-\frac{N}{N_{\star}} \right), \quad (12)$$

where F_{\star} and N_{\star} are functions of z and $\gamma = \text{const.}$ If we specialize to the case where N_{\star} is a constant, then F_{\star} contains all of the z -dependence, and is proportional to dX/dz (i.e., all of the redshift dependence is due to the cosmological geometry). In this case, we may rewrite equation (11) as

$$\begin{aligned} n(z; \Omega_{\Lambda}, \eta, N_{\text{avg}}) &\equiv \int_{N_{\text{min}}}^{\infty} F_{\text{obs}}(N, z) dN \\ &= \left(\frac{c}{H_0 m_{\text{H}}} \right) \left(\frac{1}{N_{\text{avg}}} \right) \left[\frac{(1+z)^2 g(z)}{\sqrt{(1-\Omega_{\Lambda})(1+z)^3 + \Omega_{\Lambda}}} \right] \rho_{\text{s0}}(1 + \eta - f), \end{aligned} \quad (13)$$

where

$$N_{\text{avg}} \equiv \frac{\int_{N_{\text{min}}}^{\infty} F_{\text{obs}}(N, z) N dN}{\int_{N_{\text{min}}}^{\infty} F_{\text{obs}}(N, z) dN} = N_{\star} \cdot \frac{\Gamma(2 - \gamma, N_{\text{min}}/N_{\star})}{\Gamma(1 - \gamma, N_{\text{min}}/N_{\star})} \quad (14)$$

is the mean column density in the distribution, with $\Gamma(a, x) \equiv \int_x^{\infty} t^{a-1} e^{-t} dt$ the incomplete gamma function. Note that equation (13), with N_{avg} independent of redshift, applies for *any* distribution $F_{\text{obs}}(N, z)$ which is separable into functions of N and z . The assumption of separability is particularly appealing if only a small fraction of the available HI is depleted from DLA galaxies during the redshift range under consideration. Suppressing the dependence on Ω_{Λ} , η , and N_{avg} for brevity, the quantity $n(z)$ defined in equation (13) denotes the redshift distribution of absorbers; the number of systems observed with redshifts between z and $z + dz$ is $n(z)dz$.

For the moment, assume that we know the *shape* of $F_{\text{obs}}(N, z)$ a priori, and hence that we know N_{avg} from equation (14). [We will address the question of how to incorporate properly our incomplete knowledge of $F_{\text{obs}}(N, z)$ from the data into our analysis in the next section.] Then we may construct a likelihood function from equation (13) as follows. Suppose we wish to compare the data to our prediction over a range of redshifts $(z_{\text{min}}, z_{\text{max}})$. If we divide this range into sufficiently small intervals dz , such that $n(z)dz \ll 1$, then there will be at most one object in each such interval. Then the probability of finding no objects in a given interval at a redshift z is given by the Poisson distribution, $P(0) = \exp[-n(z)dz]$; similarly, the probability of finding one object is $P(1) = n(z)dz \exp[-n(z)dz]$; and the probability of finding more than one object is negligible, $\sum_{i=2}^{\infty} P(i) \sim O\{[n(z)dz]^2\} \ll 1$. Then the likelihood, or conditional probability of obtaining a particular data set D from a distribution $n(z)$ predicted by (13) is

$$P(D|\Omega_{\Lambda}, \eta, N_{\text{avg}}) = \left\{ \prod_{i=1}^{m_{\text{obs}}} n(z_i) dz \exp[-n(z_i)dz] \right\} \left\{ \prod_{j=1}^{m_{\text{none}}} \exp[-n(z_j)dz] \right\}, \quad (15)$$

where m_{obs} is the number of DLA systems observed, z_i is the redshift of the i -th system, m_{none} is the number of intervals dz in our range $(z_{\text{min}}, z_{\text{max}})$ which have *no* DLAs in them [note that

$m_{\text{obs}} + m_{\text{none}} = (z_{\text{max}} - z_{\text{min}})/dz]$, z_j is the redshift of the j th such interval, and we have suppressed the dependence of $n(z)$ on the parameters $(\Omega_\Lambda, \eta, N_{\text{avg}})$ for brevity. For $dz \ll 1$, equation (15) may be written as

$$P(D|\Omega_\Lambda, \eta, N_{\text{avg}}) = \left[\prod_{i=1}^{m_{\text{obs}}} n(z_i) dz \right] \exp \left[- \int_{z_{\text{min}}}^{z_{\text{max}}} n(z) dz \right]. \quad (16)$$

This probability clearly depends on the chosen size of the interval dz , and shrinks to zero as $dz \rightarrow 0$. This reflects the fact that, as dz shrinks, the number of possible distinct outcomes D increases, so the probability of obtaining any *particular* data set D goes to zero. In the next section, we will use Bayesian inference to construct confidence intervals from the likelihood function (16).

3.2. Computing Confidence Regions with Bayesian Inference

Equation (16) gives the probability of obtaining our DLA sample as a random realization of the redshift distribution (13), *assuming* the truth of a particular cosmology Ω_Λ and evolution model η , and assuming knowledge of the expected average column density N_{avg} in the sample. However, our evolution model for $\rho_{\text{HI}}(z)$ does not make any predictions about the value of N_{avg} ; we must make use of the DLA sample to extract information about the range of reasonable values for N_{avg} . In addition, the value of ρ_{s0} is uncertain since it is related to the uncertain mass-to-light ratios of present-day galaxies. Both of these uncertainties in our knowledge may be rigorously incorporated into our analysis if we use Bayesian inference.

Bayes' Theorem follows trivially from the axioms of probability and the definition of conditional probability. The theorem relates $P(\Omega_\Lambda, \eta|D, N_{\text{avg}})$, the conditional probability distribution for values of the model parameters given the observed data and an assumed value of N_{avg} , to the likelihood $P(D|\Omega_\Lambda, \eta, N_{\text{avg}})$ [cf. eq. (16)]. The conditional probability of obtaining the observed data set as a random realization of the model with particular parameter values is,

$$P(\Omega_\Lambda, \eta|D, N_{\text{avg}}) = A \cdot P(\Omega_\Lambda, \eta|N_{\text{avg}}) P(D|\Omega_\Lambda, \eta, N_{\text{avg}}). \quad (17)$$

Here, $P(\Omega_\Lambda, \eta|N_{\text{avg}})$ is the *prior* probability distribution for the two parameters, which, in the absence of any previous data, we take to be uniform and independent of N_{avg} ; and A is a normalization constant which ensures that $\int P(\Omega_\Lambda, \eta|D, N_{\text{avg}}) d\Omega_\Lambda d\eta = 1$. Note that the value of dz in equation (16), which may be taken to be arbitrarily small, is absorbed into A . Unfortunately, our *a priori* knowledge does not tell us the precise value of N_{avg} . However, we may include as an additional component of our model the assumption that the data are well fitted by a gamma distribution (12). By fitting a functional form (12) to the data, we may obtain a prior distribution $P(N_{\text{avg}})$ of reasonable values of N_{avg} . The procedure for obtaining $P(N_{\text{avg}})$ is identical to the procedure we employ to get $P(\Omega_\Lambda, \eta|D, N_{\text{avg}})$. Note that the gamma distribution is not the only plausible functional form to fit to the data; however, it provides a better fit than a single power

law (Storrie-Lombardi, Irwin, & McMahon 1996), since there is a significant break in the observed slope of $F(N, z)$. Any other reasonable two-parameter distribution (e.g. a broken power law) will yield similar results to the gamma distribution.

The sum rule of probability theory allows us to “marginalize” the parameter N_{avg} by integrating equation (17) over values of N_{avg} , weighted by $P(N_{\text{avg}})$:

$$P(\Omega_\Lambda, \eta|D) = A \cdot \int_0^\infty P(N_{\text{avg}}) P(D|\Omega_\Lambda, \eta, N_{\text{avg}}) dN_{\text{avg}}, \quad (18)$$

where we have assumed that $P(\Omega_\Lambda, \eta|N_{\text{avg}})$ is uniform, and have absorbed all constants into A such that $P(\Omega_\Lambda, \eta|D)$ is still normalized to unit area. We may incorporate the uncertainty in ρ_{s0} in a similar way. As will be seen in §4.1, the uncertainty in ρ_{s0} is approximately Gaussian. Then, making the dependence on ρ_{s0} explicit, we finally have

$$P(\Omega_\Lambda, \eta|D) = A \cdot \int_0^\infty dN_{\text{avg}} \int_0^\infty d\rho_{s0} P(N_{\text{avg}}) \exp\left[-\frac{(\rho_{s0} - \bar{\rho}_{s0})^2}{2\sigma^2}\right] P(D|\Omega_\Lambda, \eta, N_{\text{avg}}, \rho_{s0}), \quad (19)$$

where once again the normalization has been absorbed into A . We will use equation (19), substituting equations (13) and (16) for $P(D|\Omega_\Lambda, \eta, N_{\text{avg}}, \rho_{s0})$ and obtaining $P(N_{\text{avg}})$ from a fit to the data, to compare the data to the models and calculate confidence regions.

4. Results: Application to the DLA Sample

We include in our sample all DLA systems whose redshifts and HI column densities (or, in a few cases, equivalent widths) have appeared in the literature (Wolfe et al. 1986; Lanzetta 1991; Lanzetta 1995; Wolfe et al. 1995; Storrie-Lombardi, McMahon, & Irwin 1996), for a total of 73 systems. In the cases where no HI column density has been confirmed, we have calculated it from the reported equivalent width using equation (3) in Wolfe et al. (1986). This is the same sample used by Storrie-Lombardi, McMahon, & Irwin 1996, with the addition of data from Wolfe et al. (1995). In our analysis, we have concentrated on high redshifts ($z > 2$), and hence have used subsets of this sample.

4.1. Calculating the Present-Day Stellar Density ρ_{s0}

Since our final results depend sensitively on the value and degree of uncertainty in the local stellar density ρ_{s0} , it is important that we obtain the most accurate and precise possible estimate of this quantity from the literature. Previous studies (Wolfe et al. 1995; Lanzetta et al. 1995; Storrie-Lombardi, McMahon, & Irwin 1996) have employed the value $\rho_{s0}/\rho_c = 2.7 \times 10^{-3 \pm 0.18} h^{-1}$ (Gnedin & Ostriker 1992), where $\rho_c \equiv 3H_0^2/8\pi G$ is the present-day critical density, and the Hubble constant is $H_0 = 100h$ km s⁻¹ Mpc⁻¹. We make use of recent observations to refine this estimate.

We compute ρ_{s0} by multiplying the local luminosity density of galaxies by their mean stellar mass-to-light ratio. Since the mass-to-light ratio is in general correlated with the galaxy luminosity, we have

$$\rho_{s0} = \int_0^\infty \phi(L)\Upsilon(L)LdL, \quad (20)$$

where $\phi(L)$ is the galaxy luminosity function (LF) and $\Upsilon(L)$ is the mass-to-light ratio in solar units. We have used the luminosity function for the NS112 sample of the Las Campanas redshift survey (Lin et al. 1996), which represents the most precise determination of the local LF to date. We include all galaxy types, since recent identifications of DLA galaxies (Le Brun et al. 1996) have indicated that DLA systems may be associated with a wide range of morphological types. Lin et al. (1996) obtain a best-fit Schechter function with the parameters $M_* = -20.29 \pm 0.02 + 5 \log h$, $\alpha = 0.70 \pm 0.03$, and $\phi_* = (0.019 \pm 0.001)h^3 \text{ Mpc}^{-3}$, where the photometry was done in a band very similar to the Cousins R_c band. Lin (1997, private communication) points out that these Schechter parameters also provide a good fit for the Gunn r -band luminosity function after a correction is made from isophotal to total galaxy magnitudes. Using a solar absolute magnitude of $r = 4.83$ (Broeils, 1997, private communication), this yields an r -band luminosity density of $j_r = (1.9 \pm 0.1) \times 10^8 h L_\odot \text{ Mpc}^{-3}$. For the mass-to-light ratio $\Upsilon(L)$, we use the relation measured by Broeils & Courteau (1996) in the Gunn r -band for the disks of Sbc-type galaxies: $\Upsilon(L) = [5.8(L/10^{10} L_\odot)^{0.24} \pm 1]h$, where the uncertainty is the 1σ deviation and the distribution of observed values is approximately Gaussian. Thus, the uncertainty in ρ_{s0} is dominated by the Gaussian uncertainty in $\Upsilon(L)$. We include all galaxy types in our calculation of ρ_{s0} , with the assumptions that spiral galaxies are well described by maximal-disk models, and that spiral and elliptical galaxies have the same stellar mass-to-light ratio. We take the mass-to-light ratio for Sbc galaxies as typical for all galaxy types of the same luminosity. Our approach overestimates the stellar mass-to-light ratio somewhat if, as some studies suggest (Rix et al. 1997), the dark matter accounts for a significant fraction of the total mass in the inner regions of galaxies. Using equation (20), we obtain

$$\frac{\rho_{s0}}{\rho_c} = (4.0 \pm 1.0) \times 10^{-3} h^{-0.48}. \quad (21)$$

Based on the uncertainty in $\Upsilon(L)$, we assume that the values of ρ_{s0} are normally distributed with a variance $\sigma = 1.0 \times 10^{-3} h^{-0.48}$.

4.2. Effects of Dust

The observed column density distribution of DLA systems, and hence the inferred value of ρ_{HI} , is affected by the presence of dust in the DLA galaxies (Fall & Pei 1993). The dust obscures background QSOs, and causes incompleteness in the DLA sample. The presence of dust leads to an underestimate of ρ_{HI} from the data; accounting for this fact will lead to better agreement between data and predictions for high- Λ cosmologies. Fall & Pei (1993) showed that the true

column density distribution is given by

$$F_{\text{true}}(N, z) = F_{\text{obs}}(N, z) \exp[\beta\tau(N, z)], \quad (22)$$

where β is the power-law slope at the bright end of the QSO luminosity function [$\phi(L) \propto L^{-(\beta+1)}$], and τ is the extinction optical depth, given by

$$\tau(N, z) = k(z) \left(\frac{N}{10^{21} \text{cm}^{-2}} \right) \xi \left(\frac{\lambda_e}{1+z} \right). \quad (23)$$

Here, $k(z) = \rho_d/\rho_g$ is the dimensionless dust-to-gas ratio, ξ is the extinction curve, and λ_e is the effective wavelength of the band of the QSO survey. We have used equations (22) and (23), together with an assumption that the observed distribution $F_{\text{obs}}(N, z)$ may be fit by a gamma distribution (12), and that $k(z)$ is proportional to the metallicity, to estimate the correction to the expected value of $\rho_{\text{HI}}(z)$ due to dust obscuration. Following Pei & Fall (1995), we assume that $k(0) = 0.8$, $\beta = 2$, and $\xi(\lambda) = \lambda_B/\lambda$ for QSO surveys in the B -band. We assume that the metallicity at redshifts $z = 3 \pm 1$ is approximately one-tenth of the solar value, $Z(z = 3 \pm 1) = 0.1Z_{\odot}$. We find that the effect of dust is to reduce the inferred value of ρ_{HI} by a factor of ~ 1.5 . Our results in the next section will include this correction.

4.3. Results of Bayesian Analysis

We have applied equation (19), corrected for dust extinction, to the DLA sample for two redshift ranges, $2 < z < 4$ and $2.5 < z < 3.5$, allowing $0 \leq \Omega_{\Lambda} \leq 1$, $-1 \leq \eta \leq 1.5$. To compute the prior distribution $P(N_{\text{avg}})$, we first fit a gamma-distribution (12) to the data, and use Bayesian methods similar to those described in §3.2 to obtain a probability distribution $P(\gamma, N_{\star})$. We fix F_{\star} by requiring that the integral of $F_{\text{obs}}(N, z)$ over all column densities be equal to the total number m_{obs} of DLAs observed in the narrow redshift interval under consideration. We then obtain a cumulative probability distribution for N_{avg} by integrating numerically the probability $P(\gamma, N_{\star})$ inside contours of constant N_{avg} in the (γ, N_{\star}) plane, given by equation (14). We differentiate this cumulative distribution numerically to obtain the differential distribution $P(N_{\text{avg}})$. Finally, we use equations (13) and (16) to obtain the likelihood function $P(D|\Omega_{\Lambda}, \eta, N_{\text{avg}}, \rho_{s0})$. Substituting these results into equation (19) gives the differential probability distribution $P(\Omega_{\Lambda}, \eta|D)$. Confidence regions are obtained by integrating this distribution inside contours of constant $P(\Omega_{\Lambda}, \eta|D)$. Our results do not depend strongly on the value of the Hubble constant; we assume $H_0 = 70 \text{ km s}^{-1} \text{ Mpc}^{-1}$.

In figure 1a, we show 68%, 95%, and 99% confidence regions in the (Ω_{Λ}, η) plane, for the redshift range $2 < z < 4$; figure 1b shows the same for the redshift range $2.5 < z < 3.5$. In both cases, we assume that 25% of the present-day mass density in stars had been assembled by $z = 2$ ($f = 0.25$), consistent with the star formation rate of Madau (1996). The effect of the sample size is evident: the 99% confidence region is 20% smaller for the larger sample (45 objects with

$2 < z < 4$) than for the smaller sample (17 objects with $2.5 < z < 3.5$). Note that, for the larger sample, the data are inconsistent with a net expulsion of more than half of the gas from galaxies ($\eta > 1$) at the 99% confidence level, and also rule out $\eta > 0.5$ at 95% confidence and $\eta > 0.1$ at 68%, in all flat cosmologies. One may compare this result with the observational finding that the intracluster medium (ICM) in rich clusters of galaxies contains an amount of iron which is approximately equal to the amount found in the stellar component of galaxies in these clusters (Renzini et al. 1993; Loewenstein & Mushotzky 1996). The natural explanation is that the iron in the ICM was produced in supernova explosions inside of galaxies, and was subsequently expelled into the ICM by supernova-driven winds. If galaxies were fully assembled by a redshift $z \sim 4$, then they should have had twice as much baryonic material at such redshifts than is observed locally. Since our analysis excludes the possibility that there was more than 1.5 (1.75) times the present-day baryonic density at 95% confidence for the larger (smaller) samples, it suggests that (1) infall of material into existing galaxies or formation of new galaxies has taken place since $z = 2$; or (2) more than 25% by mass of the present-day stellar population formed by $z = 2$. These possibilities will be discussed in more depth in §5. Note also that for high- Ω_Λ cosmologies, outflow models are strongly ruled out, so it would be more difficult to reconcile the DLA data with the intracluster iron observations in an Ω_Λ -dominated universe.

If we wish to specialize to a particular cosmological model, we should consider the one-dimensional probability distribution $P(\eta|D, \Omega_\Lambda)$, since the sizes of the confidence intervals decrease when the number of free parameters is reduced. Figure 2a shows the probability distribution for η , given $\Omega_\Lambda = 0$ (the case corresponding to the most conservative constraints on η). We consider the sample with $2 < z < 4$. The solid curves correspond to different assumptions about the amount of star formation that took place at $z > 3 \pm 1$: $f = 0, 0.25, \text{ and } 0.5$, from left to right. Upper limits on η derived from these curves are summarized in Table 1. As f increases, the gas density observed in DLAs is supplemented by more and more stars, so the data become more consistent with the closed-box model. As can be seen from Figure 2a, the data are consistent with modest to significant amounts of infall or formation of new galaxies subsequent to $z \approx 3$. Significant expulsion is less likely; for $f = 25\%$ the data are inconsistent with $\eta > 0.42$ at 95% confidence. If one allows for half of the present-day stellar population to form before $z = 3$, then one achieves marginal consistency with $\eta = 0.92$ at 95% confidence. However, in this case the metallicity of DLA systems will significantly exceed its observed value of $0.1Z_\odot$ at $z \gtrsim 2$ (Lu et al. 1996). Figure 2b shows similar results for $\Omega_\Lambda = 0.7$; here, no significant amount of expulsion is viable. Hence, it is unlikely that all of the baryonic material seen today in galaxies and the ICM of rich clusters was present in DLA galaxies at redshifts $z > 2$. The dotted curves in Figure 2 are the results obtained by considering present-day galaxies + ICM as a whole, with equal mass densities in stars and the ICM. Hence, we attempt to account for an amount “ $\rho_{\text{b,gal}}(0)$ ” = $2\rho_{\text{s}0}$. We assume that 25% of the present-day mass in stars + enriched ICM (that is, $0.5\rho_{\text{s}0}$) was present in the form of stars by $z = 2$. Clearly, only about half of this amount was present in DLA galaxies at $z > 2$ (see Fig. 2); the rest of it must have assembled into galaxies (and some of it subsequently expelled) after $z = 2$. This possibility will be discussed further in §5.

The constraints obtained with our method will improve as the catalog of DLA systems grows. The Sloan Digital Sky Survey, which is getting underway in 1997 (Gunn & Knapp 1993; see also <http://www.astro.princeton.edu/BBOOK>), will catalog $\sim 10^5$ quasars, at least an order of magnitude more than the number discovered to date (Loveday 1996). Spectroscopic follow-ups on this sample could increase the DLA sample size by 1–2 orders of magnitude. In Figure 3, we predict the effect on our results of a more modest increase in the DLA sample size. Figure 3a indicates how the probability distribution $P(\eta)$ changes when the sample size m_{obs} with $2.5 < z < 3.5$ is increased by a factor of 2 or 5. For illustrative purposes, we choose $\Omega_\Lambda = 0$ and $f = 0.25$. We take into account the observational uncertainty σ in the present-day stellar density ρ_{s0} , and assume that the additional DLAs have the same column density distribution as the existing sample. In this case it is a simple analytical matter to determine $P(\eta)$ for a hypothetically larger data set. The trend is obvious: as more data are acquired, our measurement of η becomes more precise, and $P(\eta)$ becomes more sharply peaked. Given our assumptions, the mean value of η will remain constant, but the confidence intervals will shrink. For the case shown in Figure 3a, the 95% upper bound on η is 0.32, 0.10, and -0.08, respectively, for $m_{\text{obs}} = 17, 34, \text{ and } 85$. In reality, the mean value of η will shift around as the column density distribution becomes better known [i.e. N_{avg} in equation (14) will not remain constant as observations improve], but the width of $P(\eta)$ will still behave in the same way. The precision with which we can measure η is limited by the 25% uncertainty in ρ_{s0} . Figure 3b demonstrates what would happen if ρ_{s0} were known exactly. In this case, the statistics are purely Poisson and the width (and hence the height) of our normalized distribution scales as $(m_{\text{obs}} + 1)^{1/2}$.

5. Summary and Conclusions

We have used the catalog of DLA systems to place constraints on the amount of evolution in the baryonic content of galaxies and the value of the cosmological constant. We compared the gas density ρ_g at redshift $z = 3 \pm 1$ to the present-day stellar mass density ρ_{s0} in galaxies for a range of flat cosmologies with $\Omega_\Lambda + \Omega_m = 1$. Our underlying assumption is that cold gas is required for star formation. We make use of the facts that DLA systems dominate the HI content of the universe at redshifts $z > 2$ and the correction to their baryonic mass due to molecular gas is small, $\lesssim 20\%$ (Ge & Bechtold 1997).

We defined η to be the net fraction of the baryonic content of local galaxies which was expelled since $z \approx 3 \pm 1$, and used Bayesian inference to derive confidence regions in the (η, Ω_Λ) plane. In all cosmologies we find that $\eta < 0.4$ with at least 95% confidence, as long as only $< 25\%$ of the current stellar population formed before $z = 3$. The most likely value of η is negative (cf. Fig. 2), implying a net *increase* by several tens of percent in the baryonic mass of galaxies since $z \approx 3$. The inferred value of η is more extreme for Ω_Λ -dominated cosmologies. On the other hand, recent observations of high metal abundances in the intracluster medium of rich clusters (Renzini et al. 1993; Loewenstein & Mushotzky 1996) require that metal-rich gas be *expelled* from galaxies

in an amount approximately equal to the current mass in stars. The possibility that a dominant fraction of the present-day stellar population may have already formed by $z = 3$ and resulted early on in this expulsion, is ruled out by the low metallicities (0.01–0.1 solar) observed in DLAs at $z \gtrsim 3$ (Lu et al. 1996). Moreover, the intergalactic medium which later accretes onto clusters of galaxies has a metallicity as low as $\sim 10^{-2}$ solar at $z \gtrsim 2$ (Cowie et al. 1995; Tytler et al. 1995; Songaila & Cowie 1996; Cowie 1996), rather than the needed value of ~ 0.3 solar. Most of the required metal enrichment and star formation activity must therefore have occurred at $z \lesssim 2$.

The most likely explanation to the above discrepancy is that a significant amount of gas had been assembled and partly expelled from galaxies after $z = 2$. The increase in galactic mass could have been either in the form of accretion onto existing galaxies or through the formation of new galaxies, such as those responsible for the faint excess in deep galaxy counts (Lowenthal et al. 1996, and references therein). The likely value of η of minus several tenths (Fig. 2), implies that more than half the associated baryonic mass was processed through galaxies after $z = 2$. As an example, let us assume that $\eta = -0.5$ at $z = 3 \pm 1$, and that 150% of the current baryonic mass of galaxies had assembled after $z = 2$. This implies that the total mass processed through galaxies is twice (150%+50%) their current mass, as required by the observation that clusters contain twice the iron locked up in stars (Renzini et al. 1993; Elbaz, Arnaud, & Vangioni-Flam 1995; Lowenstein & Mushotzky 1996). Half of the processed mass was converted into galactic stars and half expelled into the intergalactic medium. If the expelled gas is $\sim 10\%$ of the intergalactic gas it mixed with [assuming $\Omega_b \sim 5\%$ and the value of ρ_{s0} in Eq. (21)], then it could have yielded the ~ 0.3 solar metallicity observed in clusters as long as its original metallicity was a few times solar. The phase of massive metal enrichment must have occurred at $z \sim 0.5$ –2 since the iron abundance in clusters shows little evolution at $z \lesssim 0.5$ (Mushotzky & Lowenstein 1997). This inference could be tested observationally through a dedicated search for enhanced star formation activity and supernova rate at $z \sim 0.5$ –2.

We have employed a Bayesian analysis which has the dual advantages of taking the various observational uncertainties properly into account, and making use of unbinned data. The constraints obtained with our method will improve as the size of the quasar sample increases (cf. Fig. 3). In particular, future spectroscopic observations of the $\sim 10^5$ quasars cataloged by the Sloan Digital Sky Survey (<http://www.astro.princeton.edu/BBOOK>), could increase the current sample size of DLAs by 1–2 orders of magnitude, and improve our limits on the amount of galactic evolution considerably.

We thank Tom Loredo for useful comments. AL was supported in part by the NASA ATP grant NAG5-3085 and the Harvard Milton fund.

REFERENCES

- Briggs, F. H., Wolfe, A. M., Liszt, H. S., Davis, M. M., & Turner, K. L. 1989, *ApJ*, 341, 650
- Broeils, A. H., & Courteau, S. 1996, preprint astro-ph/9610264
- Cowie, L. 1996, in *HST and the High Redshift Universe*, Proc. 37th Herstmonceux conference, eds. Tanvir, N. R., Aragón-Salamanca, A., Wall, J.V. (World Scientific:Singapore), in press, (preprint astro-ph/9609158)
- Cowie, L. L., Songaila, A., Kim, T.-S., & Hu, E. M. 1995 *AJ*, 109, 1522
- Djorgovski, S. G., Pahre, M. A., Bechtold, J., & Elston, R. 1996, *Nature*, 382, 234D
- Elbaz, D., Arnaud, M., & Vangioni-Flam, E. 1995, *A & A*, 303, 345
- Fall, S. M., & Pei, Y. C. 1993, *ApJ*, 402, 479
- Frenk, C. S., Baugh, C. M., Cole, S., & Lacey, C. G. 1996, To appear in “Dark Matter 1996: Dark and Visible Matter in Galaxies and Cosmological Implications”, eds M. Persic and P. Salucci (preprint astro-ph/9612109)
- Ge, J., & Bechtold, J. 1997, *ApJ*, 477, L1, in press (preprint astro-ph/9701041)
- Gnedin, N. Yu., & Ostriker, J. P. 1992, *ApJ*, 400, 1
- Gunn, J. E., & Knapp, J. 1993, *Sky Surveys*, ed. B. T. Soifer, ASP Conference Series #43, 267
- Kochanek, C. S. 1996, *ApJ*, 466, 638
- Lanzetta, K. M., Wolfe, A. M., & Turnshek, D. A. 1995, *ApJ*, 440, 435
- Lanzetta, K. M., et al. 1991, *ApJS*, 77, 1
- Le Brun, V., Bergeron, J., Boissé, P., & Deharveng, J. M. 1996, *A&A*, in press (preprint astro-ph/9611031)
- Lin, H., et al. 1996, *ApJ*, 464, 60
- Loewenstein, M., & Mushotzky, R. F. 1996, *ApJ*, 466, 695
- Lowenthal, J. D., Koo, D. C., Guzman, R., Gallego, J., Phillips, A. C., Faber, S. M., Vogt, N. P., Illingworth, G. D., & Gronwall, C. 1996, *ApJ*, in press (preprint astro-ph/9612239)
- Loveday, J. 1996, preprint astro-ph/9605028
- Lu, L., Sargent, W. L. W., Barlow, T. A., Churchill, C. W., & Vogt, S. 1996, *ApJS*, 107, 475
- Lu, L., Sargent, W. L. W., & Barlow, T. A. 1997, *ApJ*, in press (preprint astro-ph/9701116)
- Madau, P. 1996, preprint astro-ph/9612157
- Madau, P., Ferguson, H. C., Dickinson, M. E., Giavalisco, M., Steidel, C. C., & Fruchter, A. 1996, preprint astro-ph/9607172
- Mushotzky, R. F., & Loewenstein, M. 1997, preprint astro-ph/9702149
- Pei, Y. C., & Fall, S. M. 1995, *ApJ*, 454, 69

- Prochaska, J. X., & Wolfe, A. M. 1997, ApJ, submitted (preprint astro-ph/9605021)
- Rix, H.-W., de Zeeuw, P. T., Carollo, C. M., Cretton, N., & van der Marel, R. P. 1997, preprint astro-ph/9702126
- Renzini, A., Ciotti, L., D’Ercole, A., & Pellegrini, S. 1993, ApJ, 419, 52
- Songaila, A., & Cowie, L. L. 1996, AJ, 112, 335
- Steidel, C. C., Pettini, M., Dickenson, M., & Persson, S. E. 1994, AJ, 108, 2046
- Steidel, C. C., Bowen, D. V., Blades, J. C., & Dickenson, M. 1995, ApJ, 440, L455
- Steidel, C. C., Giavalisco, M., Pettini, M., Dickinson, M., & Adelberger, K. L. 1996, AJ, 112, 352
- Storrie-Lombardi, L. J., Irwin, M. J., & McMahon, R. G. 1996, preprint astro-ph/9608146
- Storrie-Lombardi, L. J., McMahon, R. G., & Irwin, M. J. 1996, preprint astro-ph/9608147
- Tytler, D. et al. 1995, in *QSO Absorption Lines*, ESO Astrophysics Symposia, ed. G. Meylan (Heidelberg: Springer), p.289
- Wolfe, A. M. 1995, in *QSO Absorption Lines*, ed. G. Meylan (Heidelberg: Springer), pp. 13-22
- Wolfe, A. M., Turnshek, D. A., Smith, H. E., & Cohen, R. D. 1986, ApJS, 61, 249
- Wolfe, A. M., Turnshek, D. A., Lanzetta, K. M., Lu, L., & Oke, J. B. 1992, ApJ, 385, 151
- Wolfe, A. M., Lanzetta, K. M., Foltz, C. B., & Chaffee, F. H. 1995, ApJ, 454, 698

Ω_Λ	Confidence		Upper Limits on η		
	Level	$f = 0.00$	$f = 0.25$	$f = 0.50$	(Stars + ICM) $f = 0.25$
0.0	68%	-0.30	+0.18	+0.72	-0.40
	95%	-0.06	+0.42	+0.92	-0.14
	99%	+0.20	+0.66	+1.10	+0.20
0.7	68%	-0.60	-0.32	+0.06	-0.54
	95%	-0.36	-0.06	+0.30	-0.40
	99%	-0.10	+0.18	+0.54	-0.20

Table 1: Upper limits on η for two cosmologies and different fractions $f \equiv \rho_s(3)/\rho_s(0)$ of stars formed at redshifts $z = 3 \pm 1$. The last column includes the mass density in the intracluster medium (ICM), assuming 25% of the total (stars+ICM) was in the form of stars at $z = 3 \pm 1$. See Figure 2 for the differential probability distributions $P(\eta)$ corresponding to columns 3-6.

Fig. 1.— Confidence regions in the (Ω_Λ, η) plane, computed with dust obscuration. Results are shown for two redshift intervals over which the HI density is calculated: (a) $2 < z < 4$; (b) $2.5 < z < 3.5$.

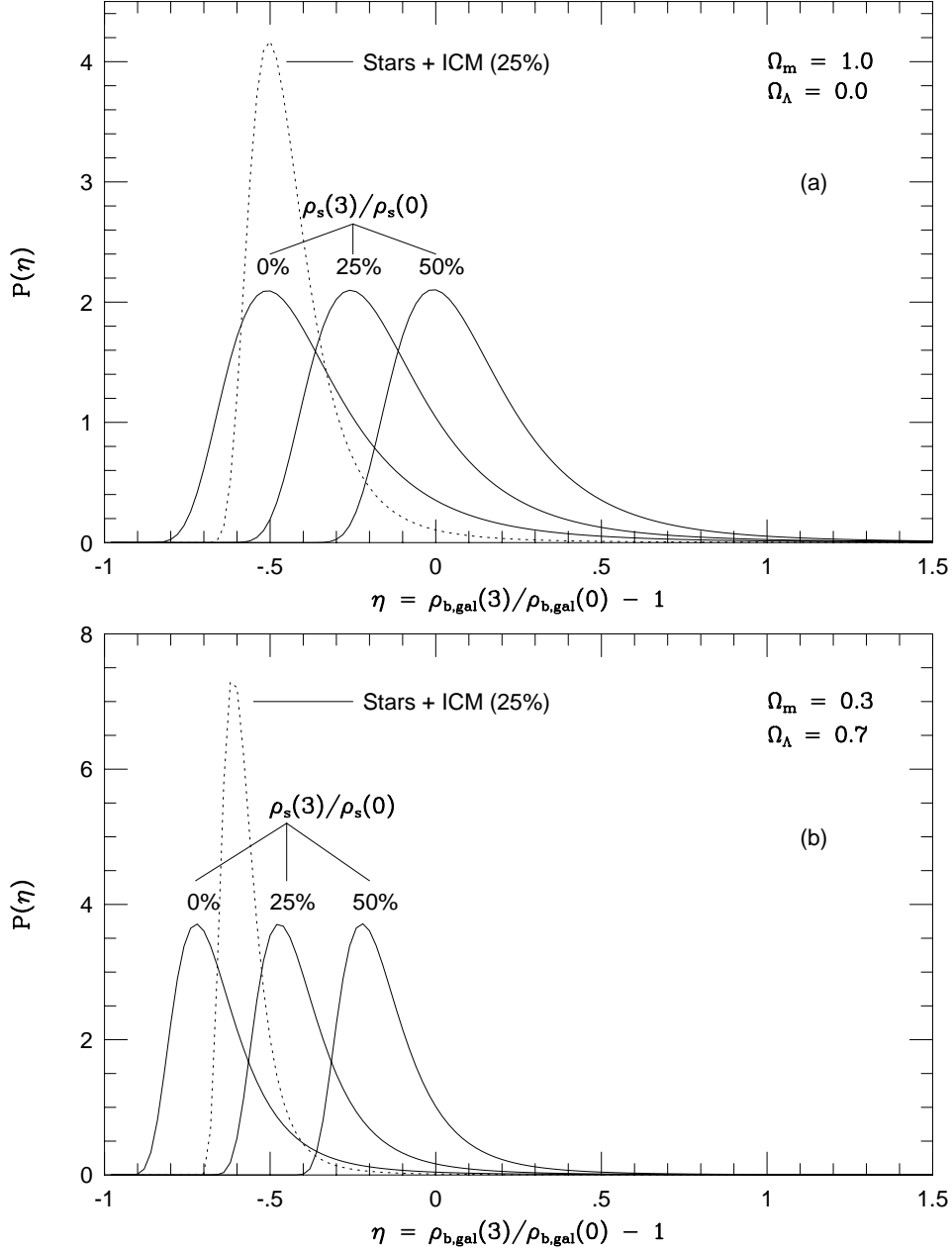


Fig. 2.— Probability distributions $P(\eta)$, for (a) $\Omega_\Lambda=0$; (b) $\Omega_\Lambda = 0.7$. We use the $2 < z < 4$ subsample. *Solid curves*: results for three different amounts of star formation before $z = 3 \pm 1$, namely 0%, 25%, and 50% of the present-day stellar density. *Dotted curves*: including the mass density in the intracluster medium (ICM), assuming 25% of the total (stars+ICM) was in the form of stars at $z = 3 \pm 1$.

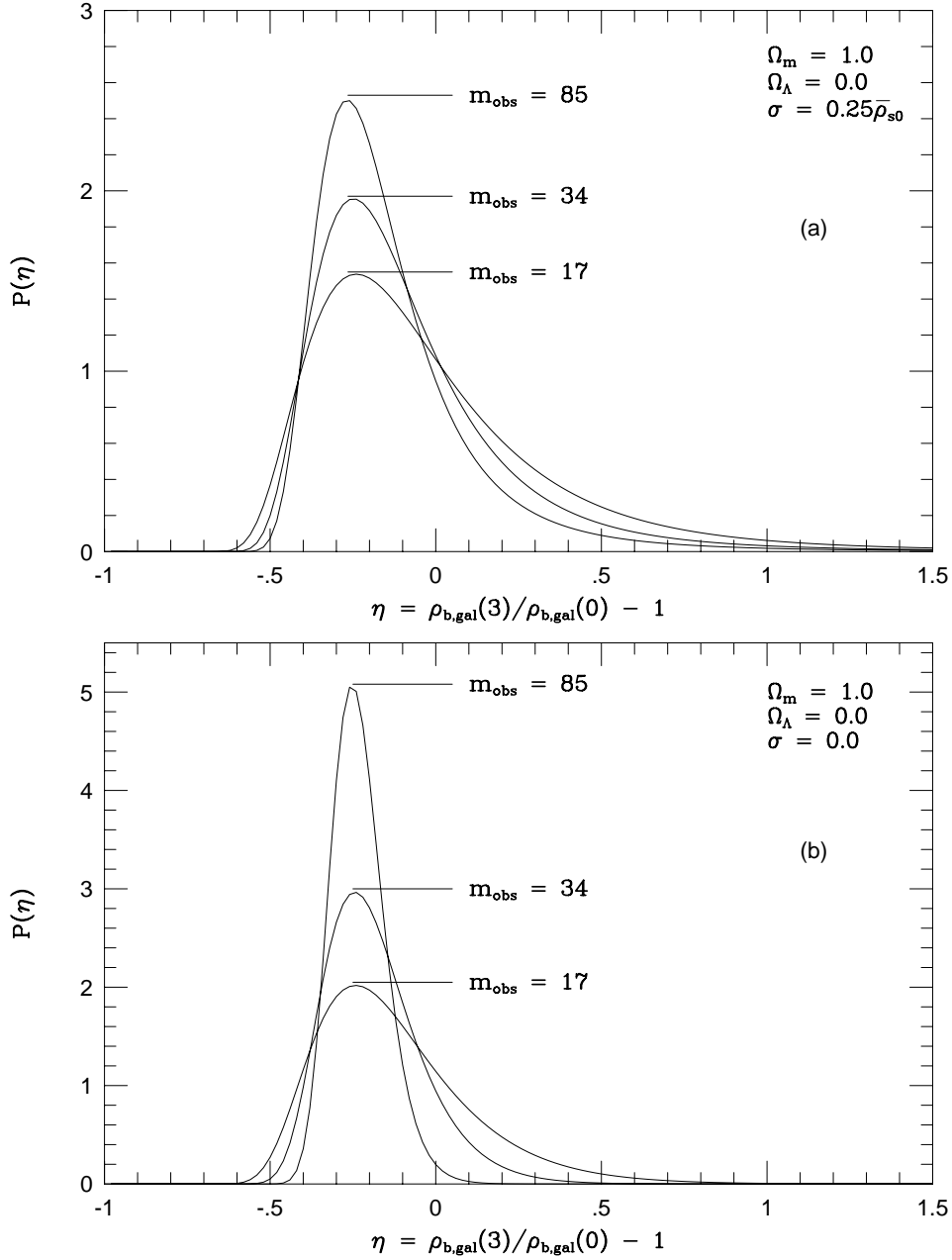


Fig. 3.— Effect of increasing the DLA sample size m_{obs} , (a) including the 25% observational uncertainty in the present-day stellar density ρ_{s0} ; (b) assuming we know ρ_{s0} exactly. We use the $2.5 < z < 3.5$ subsample.